Supplementary Material

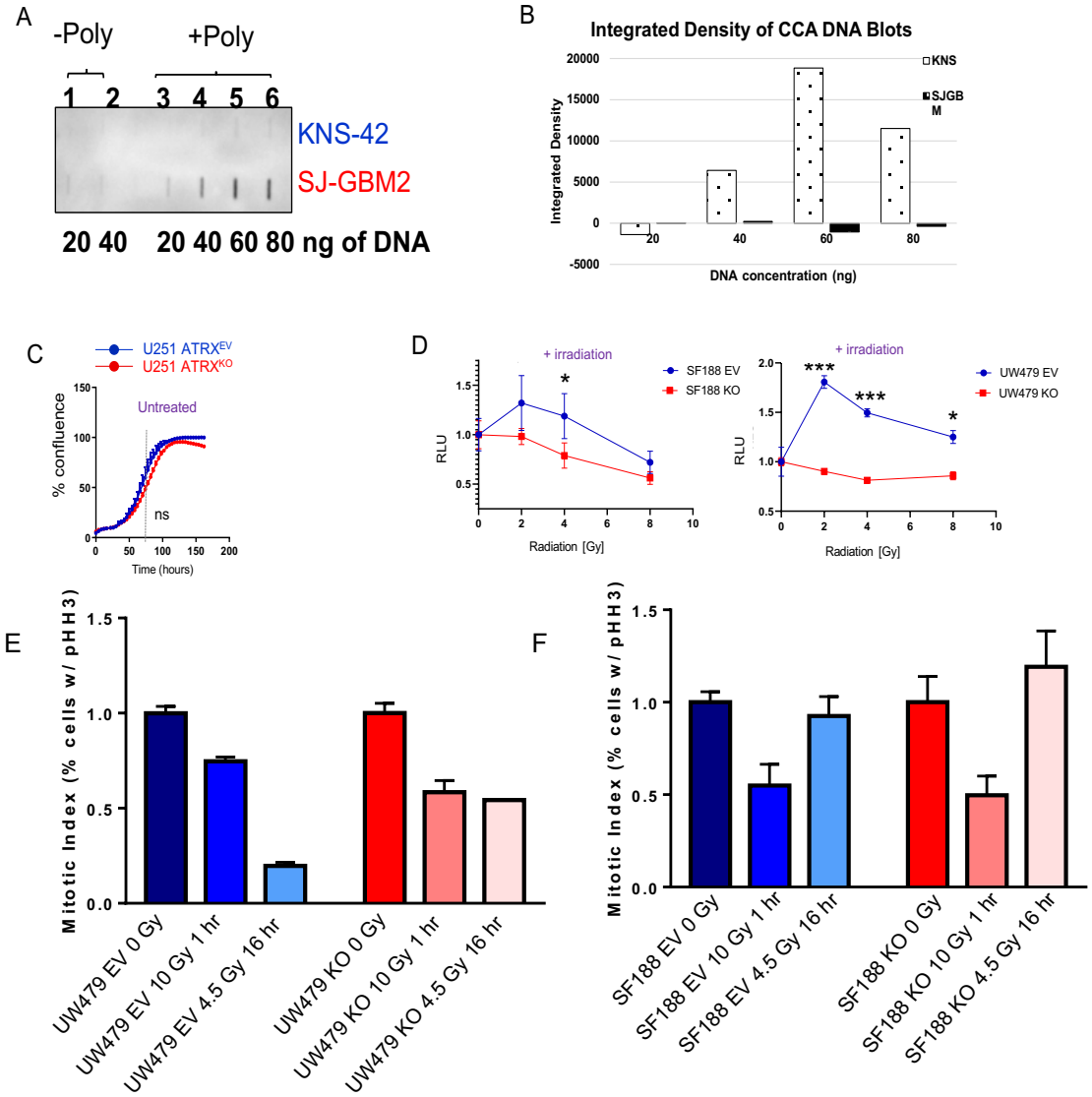

Figure S1: **Characterizing primary and isogenic pHGG cell lines based on ATRX status. Related to Figure 1.**

(**A**) Optimization of C-circle assay results demonstrating increasing amounts of DNA from each sample in the presence (+) or absence (-) of Φ29 polymerase of cells (SJ-GBM2) with established ALT. **(B)** Quantification of integrated density of band with threshold established above background significant at 40 ng DNA. (**C**) ATRX^{KO} in U251 cells does not change proliferation (n=3). (**D**) *In vitro* data showing proliferation of ATRX^{KO} SF188 and UW479 cells and their isogenic controls after exposure to increasing doses of irradiation (IR). (**E-F**) Flow cytometric analysis of phospho-histone H3 (pHH3) staining as a metric for mitotic index in isogenic UW479 and SF188 cells. Values normalized to average 0 Gy value within respective cell line. [Mean ± SEM for triplicate experiments are shown. *$P \leq 0.05$ and ***$P \leq 0.001$ using 2-Way ANOVA.]

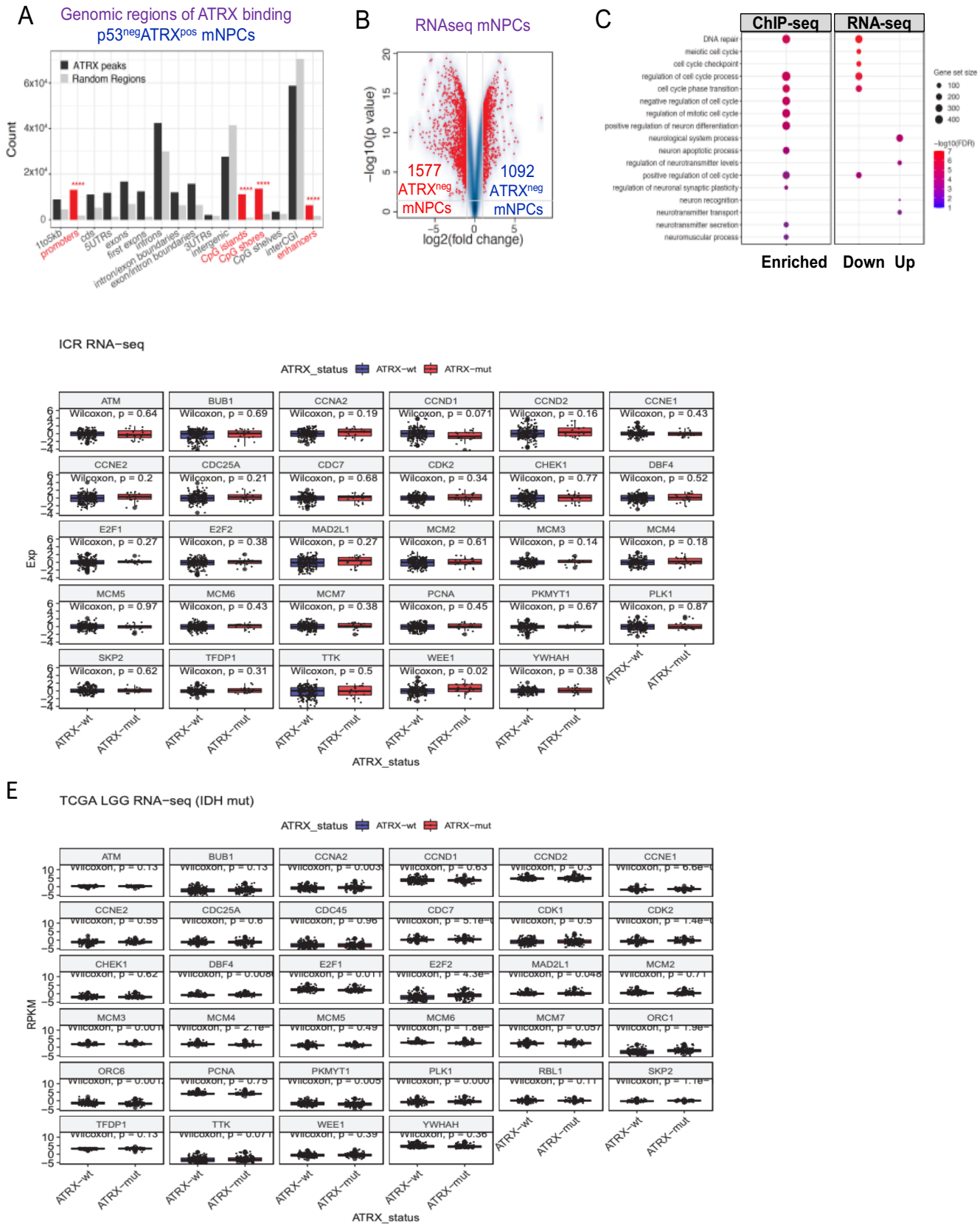
A
Genomic regions of ATRX binding
p53negATRXpos mNPCs
ATRX peaks
Random Regions
Count
B
RNAseq mNPCs
1577
ATRXneg
mNPCs
1092
ATRXneg
mNPCs
−log10(p value)
log2(fold change)
C
ChIP-seq
RNA-seq
DNA repair
meiotic cell cycle
cell cycle checkpoint
regulation of cell cycle process
cell cycle phase transition
negative regulation of cell cycle
regulation of mitotic cell cycle
positive regulation of neuron differentiation
neurological system process
neuron apoptotic process
regulation of neurotransmitter levels
positive regulation of cell cycle
regulation of neuronal synaptic plasticity
neuron recognition
neurotransmitter transport
neurotransmitter secretion
neuromuscular process
Gene set size
−log10(FDR)
Enriched
Down
Up
D
ICR RNA−seq
ATRX_status
ATRX−wt
ATRX−mut
Exp
ATRX_status
E
TCGA LGG RNA−seq (IDH mut)
ATRX_status
ATRX−wt
ATRX−mut
RPKM
ATRX_status

Figure S2: Assessment of ATRX binding and gene expression in murine and human glioma datasets. Related to Figure 2.

(**A**) Genomic region annotations of ATRX peaks in TP53$^{-/-}$ mNPCs (black bars), compared with the annotation of randomly generated regions (gray bars). The number of peaks and random regions annotated to each category of genomic regions are shown (y axis), and the enrichment of peaks at promoters, CpG islands/shores, and enhancers was evaluated using Binomial test, compared with random regions. (**B**) Volcano plot of gene expression in TP53$^{-/-}$ mNPCs RNA-seq dataset. The red dots denote significant changes in expression (genes up regulated in ATRX^{neg} in red, and up in ATRX^{pos} in blue) (FDR < 0.05 and absolute log fold change > 1). (**C**) Cell cycle and neuron-related Gene Ontology Biological Process (GOBP) terms which were enriched in ATRX binding sites (left panel, ChIP-seq) and/or up/down-regulated by ATRX status (right panel, RNA-seq, ATRX^{neg} compared to ATRX^{pos}). The color of the dots indicates the significance levels (red: lower FDR; blue: higher FDR), and the size indicates the GOBP size (the number of genes annotated to the term). **(D)** Pediatric HGG (pHGG, primarily concurrent with *H3F3A* mutation, PedcBioPortal, n=220). **(E)** Adult grade 2/3 glioma ("lower-grade" glioma, LGG, concurrent with *IDH* mutation, TCGA, n=414). [Mean ± SEM for triplicate experiments are shown. *$P \leq 0.05$, **$P \leq 0.01$, ***$P \leq 0.001$, ****$P \leq 0.0001$ using Welch's t-test.]

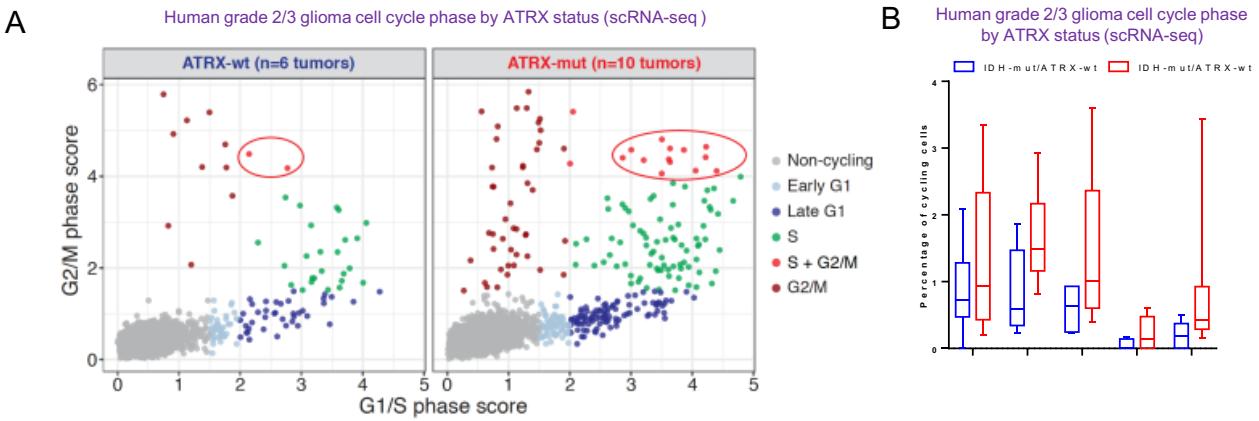

Figure S3: Comparison of cell cycle phases between ATRX-wt and ATRX-mut human glioma tumors. Related to Figure 3.

(A) Classification of non-cycling cells (black) and five phases of cycling cells based on the relative G1/S and G2/M average expression scores. Left panel: *ATRX*-wildtype gliomas ("IDH-mut/ATRX-wt", 4347 cells from 6 tumors); right panel: *ATRX*-mutant gliomas ("IDH-mut/ATRX-mut" 6341 cells from 10 tumors). Red circles denote "double positive" cells with inappropriate expression of genes associated with both S and G2/M phase. **(B)** The comparison of percentage of cycling cells at each phase between *ATRX*-wt (blue) and *ATRX*-mut (red) gliomas demonstrates increase in multiple phases including the aberrant "S+G2/M" double positive population (*$P \leq 0.05$, **$P \leq 0.01$, and ***$P \leq 0.001$ using F test for statistical variance).

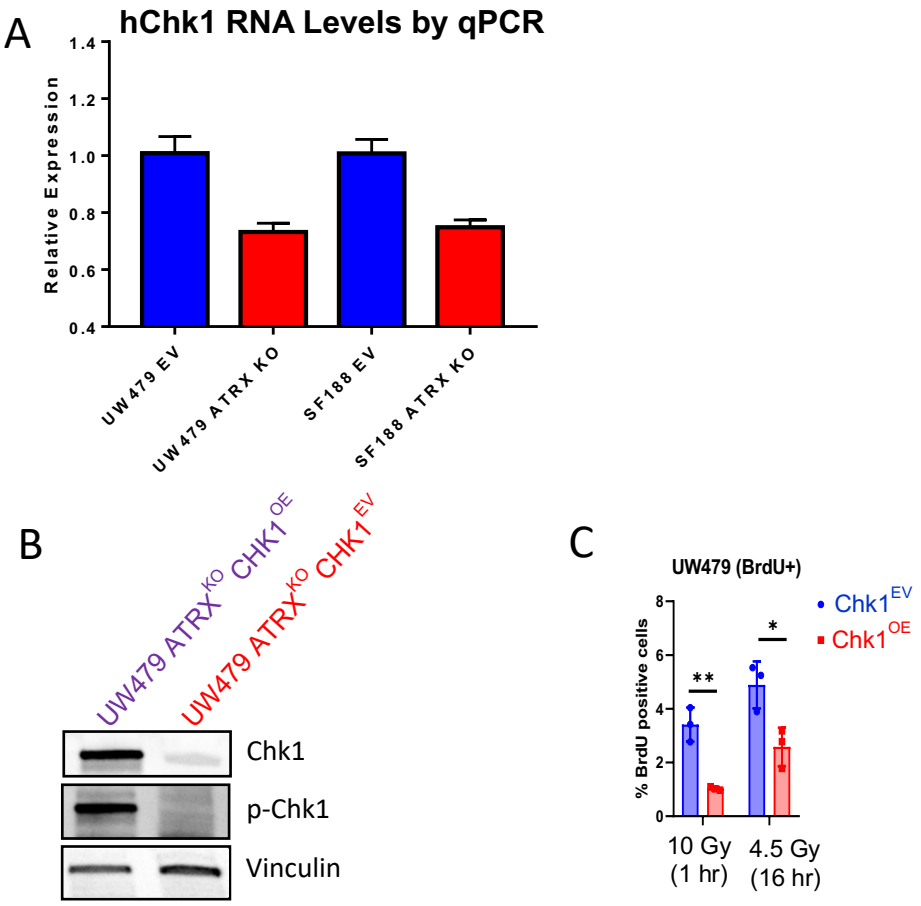

Figure S4: Analysis of Chk1 levels and effect of Chk1 overexpression on proliferation rate. Related to Figure 4.

(A) qPCR for human Chk1 show that cells with ATRX loss have decreased Chk1 at the RNA level. Normalized against GAPDH. **(B)** Chk1 expression confirmed with western blot **(C)** Proliferation rate assessed using BrdU and measured through flow cytometry. Values normalized against untreated cells within each cell line.

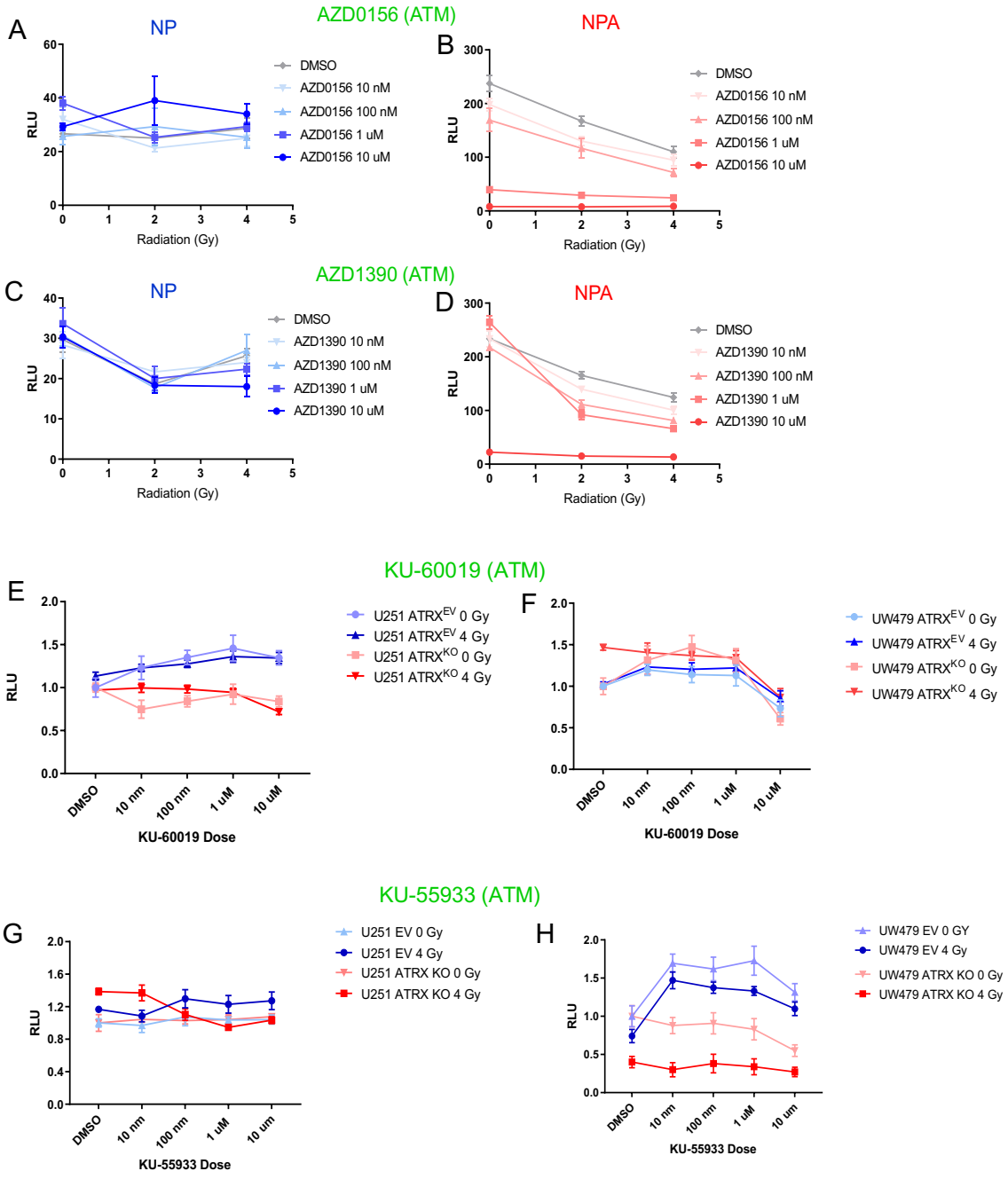

Figure S5: Cell viability assays to assess effect of ATM inhibitors with and without radiation on mouse and human glioma cells. Related to Figure 5.

(A-D) Cell viability assay of mouse GBM cells with or without ATRX knockdown plotted against dose of radiation treatment with various concentrations of ATM inhibitors. **(E-H)** Cell viability assay of isogenic human cells with or without ATRX knockdown plotted against dose of radiation treatment with various concentrations of ATM inhibitors.

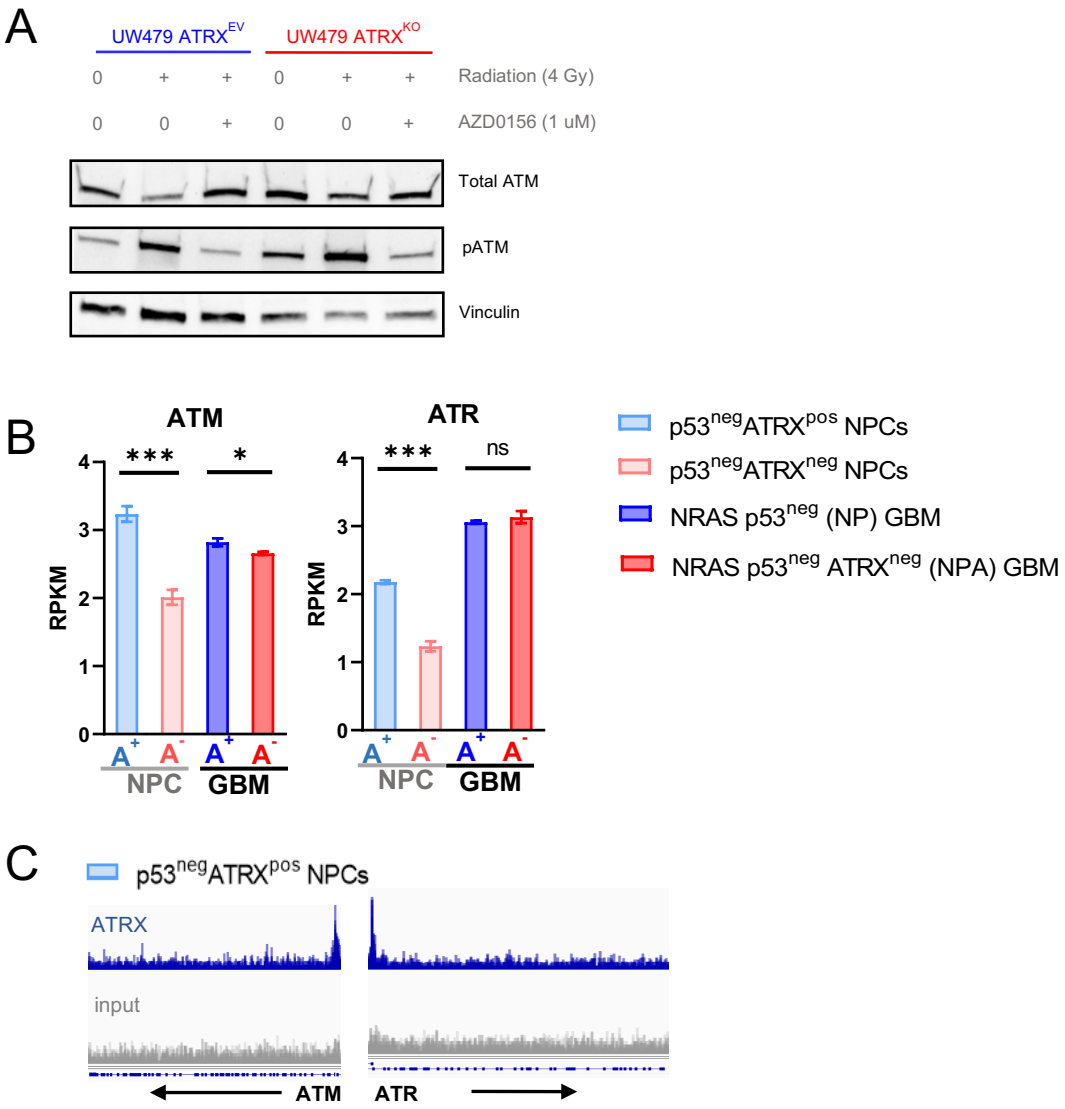

Figure S6: Assessment of ATM by western blot and ChIP-seq in human and murine gliomas. Related to Figure 5.

(A) Western blot of isogenic UW479 cells demonstrating an increase in ATM activation (pATM) in ATRX^{KO} cells after exposure to 4 Gy radiation. **(B)** Expression levels (RPKM) of ATR and ATM with isogenic loss of ATRX in mNPC and mGBM cells. [Mean ± SEM for triplicate experiments are shown. *P≤0.05, ***P≤0.001 using Welch's t-test.] **(C)** ATRX ChIP-seq tracks (n=3) in mNPC cells demonstrate ATRX promoter binding (gray track is input).

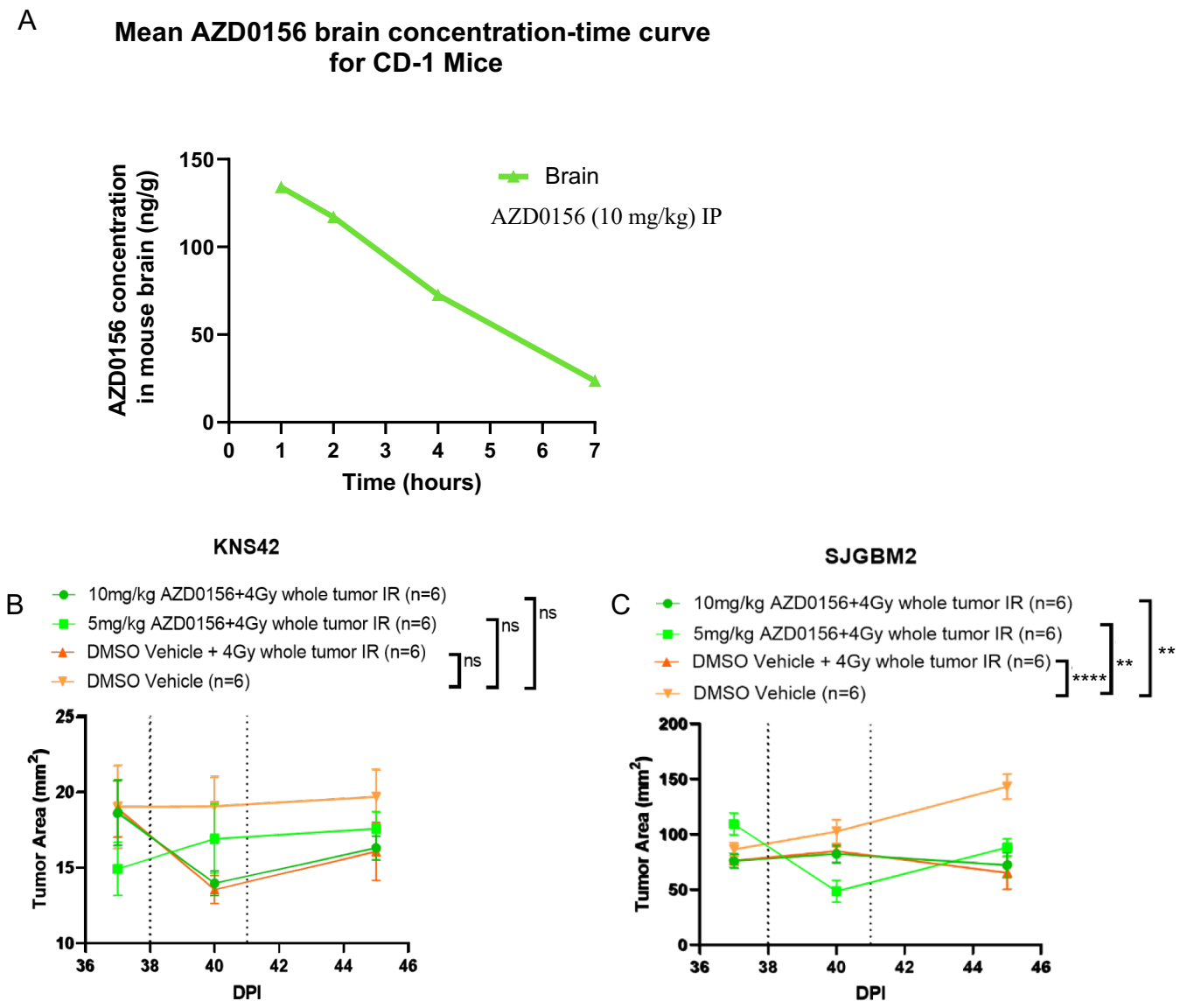

Figure S7: **Pharmacokinetics Study and Flank Tumor Growth Measurement after AZD0156 Treatment in Mice. Related to Figures 6 and 7.**

(A) Mean AZD0156 brain concentration-time curve for CD-1 Mice following an IP administration. **(B-C)** Flank tumor growth measurement in NSG mice implanted with KNS42 ATRX^{WT} and SJGBM2 ATRX^{mut} cells with different radiation and ATM inhibition treatments. [Mean ± SEM for triplicate experiments are shown. **$P \leq$ 0.01 and ****$P \leq$0.0001 using 2-Way ANOVA.]